Available online at www.sciencedirect.com
ScienceDirect
Tetrahedron Letters
Tetrahedron Letters 48 (2007) 3661–3665

Synthesis, optical, electrochemical, and thermal properties of α,α′-bis(9,9-bis-*n*-hexylfluorenyl)-substituted oligothiophenes

Vinich Promarak,* Auradee Punkvuang, Siriporn Jungsuttiwong, Sayant Saengsuwan, Taweesak Sudyoadsuk and Tinnagon Keawin

Advanced Organic Materials and Devices Laboratory, Department of Chemistry, Faculty of Science, Ubon Ratchathani University, Warinchumrap, Ubon Ratchathani 34190, Thailand

Received 13 February 2007; revised 12 March 2007; accepted 22 March 2007
Available online 25 March 2007

Abstract—A series of new α,α′-bis(9,9-bis-*n*-hexylfluorenyl)-substituted oligothiophenes with 2-, 4-, and 6-thiophene rings have been synthesized via a nickel-catalyzed reductive dimerization and their optical, electrochemical, and thermal properties investigated. The fluorene substituents have shown electronic interactions with the oligothiophene chains, enhanced the solubility of these materials and stabilized the radical cation and dication by blocking the reactive α-positions of the thiophene moieties. The absorption, fluorescence, electrochemical, and thermal properties of these materials can be tuned by varying the conjugation length of the oligothiophene segment.

Over the past few years, the study of π-conjugated organic materials has been the subject of great interest due to the increasing number of potentially active components for a wide range of electronic and optoelectronic devices.[1–3] The simple modification of the chemical structure, the solubility, and the optical properties of these organic materials makes them superior to those based on inorganic substances in terms of the manufacturing costs of the devices and the improvement in various technological aspects. In particular, oligothiophenes have been the subject of significant study due to their excellent conductivity, electroluminescent behavior, and characteristics as advanced materials for organic field effect transistors (OFETs)[4,5] and organic light-emitting diodes (OLEDs).[6,7] The advantages of π-conjugated small molecules or oligomers are that not only can they be obtained in high purity and with well-defined structures, but also, their optical, electrochemical, and thermal properties can be easily tuned by changing the structure, for example, solubilizing chains, end-capping groups, inclusion of various functional groups, and changing the oligomer lengths. A series of oligothiophenes with different terminal α,α′-substituents including aldehyde,[8] diphenylamine,[9] cyclophane,[10] pyrene,[11] bis(4-methylphenyl)aminophenyl,[12] cyclohexene,[13] ethylenedithio,[14] and phenyl[15] groups is of growing synthetic interest. Oligothiophenes terminated with fluorene moieties[16–18] have been synthesized using palladium catalyzed Suzuki and Stille coupling reactions, but due to solubility limitations, only structures up to the tetramer were prepared. These materials exhibited interesting optical and electrochemical properties and have been shown to be potential light-emitting materials in OLEDs and active components in OFETs. The synthesis and physical properties of fluorine-substituted oligothiophenes with longer oligothiophene chains and different substituents on the fluorene ring still remain to be explored. Therefore, in this Letter we report a facile synthetic approach to a series of new α,α′-bis(9,9-bis-*n*-hexylfluorenyl)-substituted oligothiophenes with 2-, 4-, and 6-thiophene rings via nickel-catalyzed reductive dimerization. Their basic optical, electrochemical and thermal properties have been investigated with the aim of understanding the structure–physical property relationships and developing novel molecular organic materials.

Scheme 1 illustrates the synthetic approach to prepare new α,α′-bis(9,9-bis-*n*-hexylfluorenyl)-substituted oligothiophenes **BFT2n** ($n = 1$–3). A reductive

Keywords: Thiophene; Fluorene; Nickel-catalyzed coupling; Oligomer; Electrochemical property; Organic light-emitting diode (OLED).
* Corresponding author. Tel.: +66 81 5930005; fax: +66 45 288379; e-mail: pvinich@sci.ubu.ac.th

0040-4039/$ - see front matter © 2007 Elsevier Ltd. All rights reserved.
doi:10.1016/j.tetlet.2007.03.131

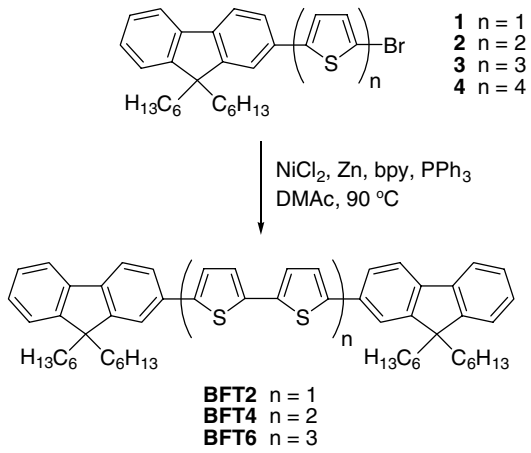

Scheme 1. The synthesis of the target oligothiophenes **BFT2n** ($n = 1$–3).

nickel-catalyzed coupling reaction was employed to dimerize the key intermediate bromo-oligothiophen-5-yl-9,9-bis-*n*-hexylfluorenes **1**, **2**, **3**, and **4** to the desired molecules **BFTn** ($n = 1$–4). Earlier, we reported the synthesis of a series of these bromo compounds involving the use of two orthogonal reactions in an iterative synthetic strategy.[19] The first reaction is a coupling to achieve growth of the oligothiophene segment. The second is a selective bromine introduction using NBS. Dimerization of the bromo-oligothiophenes **1**, **2**, and **3** with the catalytic system $NiCl_2$, zinc powder, PPh_3, and bipyridine (bpy) in DMAc at 90 °C afforded the corresponding α,α′-disubstituted oligothiophenes **BFT2** as a yellow solid, **BFT4** as an orange solid, and **BFT6** as a red solid in 47%, 40%, and 38% yields, respectively. Unfortunately, under similar conditions coupling of bromo-quaterthiophene **4** to give the corresponding octathiophene **BFT8** was unsuccessful due to the formation of an insoluble precipitate, which could not be purified by conventional chromatography techniques. This indicates the strong intermolecular interactions in the solid state for the octamer due to its nearly undisturbed π-conjugated system. Compounds **BFT2** and **BFT4** were soluble in chlorinated solvents, THF and acetone at room temperature, while **BFT6** was less soluble. Their chemical structures were confirmed by ^1H, ^{13}C NMR, FT-IR, and high resolution mass spectrometry (HRMS) analysis.[20]

To gain insight into the electronic properties and the geometries of oligomer **BFT2n** ($n = 1$–3), quantum chemical calculations were performed using the B3LYP/6-31G (d,p) method.[21] Figure 1 shows the HOMO and LUMO of **BFT6**. In the HOMO, the bonding interactions are located on the bridge C=C atoms and the antibonding interactions are located on the bridge C–C atoms. On the other hand, in the LUMO, the bonding interactions are located on the bridge C–C atoms and the antibonding orbitals are located on the bridge C=C atoms. The HOMO in **BFT6** is delocalized extensively over the whole π-conjugated system via the thiophene chain and fluorene terminal substituents, while the LUMO is delocalized through six thiophene units. Oligomers **BFT2** and **BFT4** also provided similar results. There would be a significant change in the charge distribution upon the HOMO–LUMO transition in the oligomers **BFT2n** ($n = 1$–3). The calculated HOMO–LUMO energy gaps (calcd E_g) are presented in Table 1. The results indicate that the E_g values decrease as the number of thiophene units increases. The predicted energy band gaps (calcd E_g) slightly deviate from those estimated from the onset of UV–vis absorption and the cyclic voltammogram (about 0.2 eV). There are factors that may be responsible for these errors

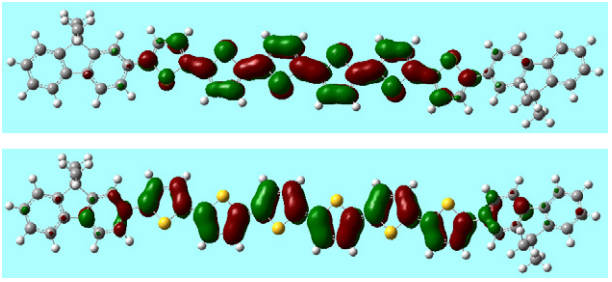

Figure 1. The HOMO (bottom) and LUMO (top) of **BFT6** calculated at the B3LYP/6-31G (d,p) level.

Table 1. Summary of the physical measurements of **BFT2n** ($n = 1$–3)

Comp	λ_{abs} (log ε)[a] nm (dm^3/mol)	λ_{em}[b] (nm)	E_g[c] (eV)	Calcd E_g[d] (eV)	Φ_F[e]	$E_{1/2}$[f] (V)	ΔE[g] (mV)	$T_c/T_m/T_{5d}$[h] (°C)	HOMO[i] (eV)	LUMO[j] (eV)
BFT2	405 (5.07), 340 (4.51)	464, 493	2.66	2.85	0.30	0.96, 1.26	300	71/126/373	−5.32	−2.66
BFT4	442 (4.84), 327 (4.43)	515	2.42	2.42	0.21	0.81, 1.02	210	112/155/418	−5.19	−2.77
BFT6	462 (4.30), 357 (3.91)	538	2.31	2.20	0.11	0.70, 0.86	160	208/231/426	−5.09	−2.78

The underlined values refer to the cooling scan.

[a] Measured in dilute CH_2Cl_2 solution.

[b] Excited at the absorption maxima.

[c] Estimated from the onset of the absorption spectra ($E_g = 1240/\lambda_{max}$).

[d] Obtained from the TDDFT/B3LYP calculation.

[e] Determined in CH_2Cl_2 solutions ($A < 0.1$) at room temperature using quinine sulfate solution in 0.01 M H_2SO_4 ($\Phi = 0.54$) as a standard.[27]

[f] Measured with a three-electrode system fitted with a platinum rod counter electrode, a glassy carbon working electrode and an SCE reference electrode in CH_2Cl_2 containing 0.1 M *n*-Bu_4NPF_6 as a supporting electrolyte at a scan rate of 50 mV/s under argon.

[g] The difference between the first and second oxidation potentials.

[h] Obtained from DSC and TGA analyses measured at a heating rate of 10 °C/min under N_2.

[i] Calculated from the empirical formula: HOMO = −(4.44 + E_{onset}).

[j] Calculated by LUMO = HOMO + E_g.

because the orbital energy difference between the HOMO and LUMO is still an approximate estimation to the transition energy since the transition energy also contains significant contributions from some two-electron integrals. In reality, an accurate description of the lowest singlet excited state requires a linear combination of a number of excited configurations.

The optical properties of the α,α′-disubstituted oligothiophenes **BFT2n** ($n = 1$–3) in dilute CH_2Cl_2 solution are depicted in Figure 2 and summarized in Table 1. The UV–vis spectra of all the compounds showed two absorption bands, which were assigned in terms of the strong absorption band at longer wavelength corresponding to the π–π* electron transition of the entire conjugated backbone and the less intense absorption bands originating from the π–π* local electron transition of the individual aromatic units. The absorption maxima of the former band of **BFT2n** ($n = 1$–3) are progressively red-shifted with increasing number of thiophene rings as the extent of the π-conjugation system in the oligomer increases, while their intensities are decreased. Compounds **BFT2n** ($n = 1$–3) exhibited the longest wavelength absorptions at 405, 442, and 462 nm, respectively, which were nearly identical to those of α,α′-bis(9,9-dialkylfluorene)-substituted bisthiophene (406 nm),[22,23] α,α′-bis(9,9-diphenylfluorene)-substituted bisthiophene (405 nm), and α,α′-bis(9,9-diphenylfluorene)-substituted quaterthiophene (440 nm).[17] However, these absorption maxima were considerably red-shifted in comparison to those of the parent unend-capped bithiophene (302 nm),[24] quaterthiophene (390 nm),[25] and sexithiophene (432 nm)[26] indicating the formation of a highly extended π-electron delocalization system through the fluorene end-caps. The HOMO–LUMO energy gaps (E_g) of **BFT2n** ($n = 1$–3) (Table 1), estimated from the onset absorption edge, decrease with the increase of the π-conjugation length of the oligothiophene segments. All α,α′-bis(9,9-bis-*n*-hexylfluorenyl)-substituted oligothiophenes **BFT2n** ($n = 1$–3) in this study are highly fluorescent with the color of the fluorescence ranging from bright yellow to bright orange. The fluorescence quantum yields (Φ_F) of the fluorescence oligomers **BFT2n** ($n = 1$–3) in dilute CH_2Cl_2 solution range from 0.11 to 0.30 (Table 1). The results indicate that the fluorescence quantum yield of the oligomers decreases with the increasing number of thiophene units. As the number of thiophene rings increases, the molecules become large, planar π-conjugated structures and they are particularly vulnerable to π-stacking. Thus with molecules that can form π-stacks there is a strong tendency toward reduced fluorescence quantum yields. The photoluminescence (PL) spectra of **BFT2n** ($n = 1$–3) showed an increasing red-shift of the maximum emission peak with an increase in the number of thiophene rings. The PL spectrum of **BFT2** is characterized by two well-defined emission peaks at 464 and 493 nm, which are similar to those of α,α′-bis(9,9-dialkylfluorene)-substituted bisthiophene (464 and 493 nm).[22,23] However, these appeared as a shoulder for compounds **BFT4** and **BFT6**. This indicates the existence of a broad distribution of the ground and excited state molecular conformations for both compounds. The large Stokes' shift (about 70 nm) between the PL and absorption maxima, and broad UV–vis absorptions (full width at half maximum around 90–107 nm) also reflect the existence of a varying twist in the ground state, whereas the excited state is more planar.

In order to investigate the electrochemical behavior of α,α′-disubstituted oligothiophenes **BFT2n** ($n = 1$–3), cyclic voltammetry (CV) measurements were performed in CH_2Cl_2 containing 0.1 M *n*-Bu_4NPF_6 as a supporting electrolyte. The results are shown in Figure 3 and summarized in Table 1. The CV curves of **BFT2**, **BFT4**, and **BFT6** demonstrated two reversible oxidation processes yielding radical cations and dications at 0.96 and 1.26 V, 0.81 and 1.02 V, and 0.70 and 0.86 V, respectively. However, under these experimental conditions, no distinct reduction process was observed in each case. As shown in Figure 3, all the thiophene oligomers gave well-defined CV curves with stable formation of both the radical cation and the dication, indicating as expected, that the fluorene substituents at the (terminal) α- and α′-positions block the reactivity of the thiophene

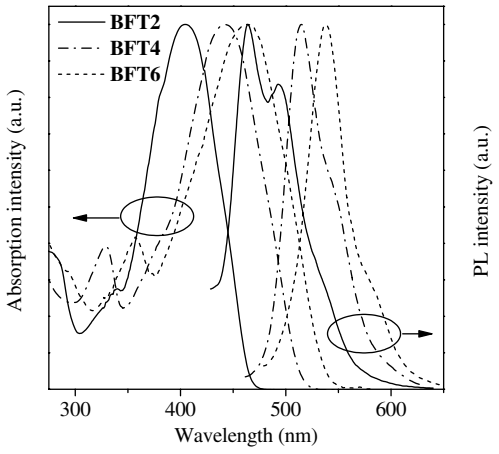

Figure 2. UV–vis absorption and photoluminescence (PL) spectra of **BFT2n** ($n = 1$–3) measured in dilute CH_2Cl_2 solution.

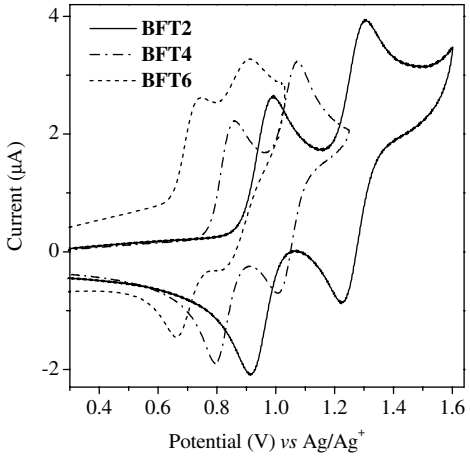

Figure 3. CV curves of **BFT2n** ($n = 1$–3) measured in CH_2Cl_2 containing *n*-Bu_4NPF_6 as supporting electrolyte at a scan rate of 50 mV/s.

moieties. Moreover, repeated cycling of the potential up to +1.6 V resulted in identical CV curves. The first oxidation potentials of **BFT2** and **BFT4** are lower than those of the parent unend-capped bithiophene[24] and quaterthiophene[25] by 0.32 and 0.18 V, respectively. Analogous to the spectroscopic results, the oxidation potentials are progressively shifted to lower energies with an increasing length of the π-conjugated system. The difference between the first and second oxidation potentials gradually decreases as the conjugation length of the oligomers increases. Potential differences between the two oxidation processes ranging from 300 to 160 mV (from **BFT2** to **BFT6**) indicate that the radical cation could efficiently delocalize the charge along the oligothiophene backbone to the fluorene end-caps. These results are consistent with the increasing red shifts in the absorption spectra. The increasing π-conjugation length is due to the extent of delocalization of the π-electron system along the backbone. However, participation of the fluorene rings in the charge delocalization becomes less important as the number of thiophene rings increases, except for interactions related to blocking of the reactive α-positions of the terminal thiophene ring and the increased solubility of the oligothiophene derivatives. The HOMO and LUMO energy levels of the oligomers were determined using the onset positions of the oxidation and energy gap (E_g) and are summarized in Table 1. The determined HOMO levels of these oligothiophenes are in the range of −5.32 to −5.09 eV, which match well with the work function of gold (Au) or indium tin oxide (ITO) electrodes, favoring injection and transport of holes.

The thermal properties of the α,α′-disubstituted oligothiophenes **BFT2n** ($n = 1$–3) were investigated by thermogravimetric analysis (TGA) and differential scanning calorimetry (DCS). The TGA and DSC results are shown in Figure 4 and are summarized in Table 1. Thermogravimetric analyses revealed that **BFT2n** ($n = 1$–3) were thermally stable materials, with onset of decomposition temperatures above 373 °C under nitrogen. As expected, the increase in number of thiophene rings resulted in an increase of the phase transition temperatures. The DSC curves of the samples of **BFT2n** ($n = 1$–3) recrystallized from CH_2Cl_2/methanol exhibited clear endothermic melting peaks (T_m) during the first heating scan at 126, 155, and 231 °C, respectively. On subsequent cooling, only compounds **BFT4** and **BFT6** were found to recrystallize with the recrystallization temperatures (T_c) being observed at 112 and 208 °C, respectively. When a non-recrystallized sample of **BFT2** was reheated, the second DSC curve showed an exothermic crystallization peak (T_c) at 71 °C followed by an endothermic peak due to melting of the same crystalline form at 126 °C. In the cases of **BFT4** and **BFT6**, only sharp endothermic melting peaks (T_m) were detected during the second heating scan at 155 and 231 °C, respectively. These results support the observation that as the number of thiophene rings increase the molecules tend to give crystalline forms due to the formation of an undisturbed π-conjugation system.

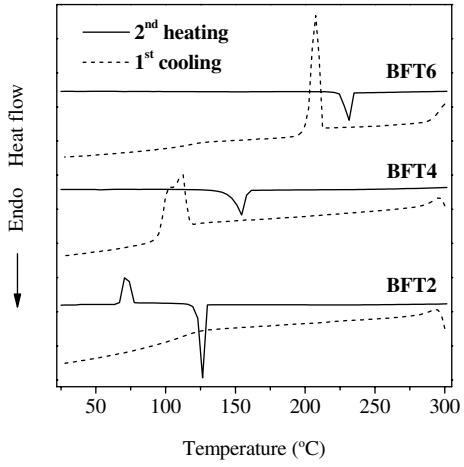

Figure 4. DSC curves (2nd heating and 1st cooling scans) of **BFT2n** ($n = 1$–3) measured at a heating rate of 10 min/°C.

In conclusion, we have presented facile synthetic procedures for the preparation of a series of new α,α′-bis(9,9-bis-*n*-hexylfluorenyl)-substituted oligothiophenes with 2-, 4-, and 6-thiophene units via a nickel-catalyzed reductive coupling reaction of bromo-oligothiophenes and their physical properties were investigated. The presence of 9,9-bis-*n*-hexylfluorene rings at both ends of the oligothiophenes had significant effects on the solubility allowing longer oligomers, up to the hexamer, to be prepared and blocking the reactive α,α′-positions of the thiophene moieties. The optical and electrochemical investigations revealed an electronic interaction between the fluorene moieties and the oligothiophene chains. The thermal properties of these materials are enhanced with the increasing number of thiophene rings. These oligothiophene derivatives display strong fluorescence and should be promising materials for OLED devices.

Acknowledgments

This research was financially supported by the National Research Council of Thailand (NRCT) and the Ubon Ratchathani University. We also thank Chulabhorn Research Institute (CRI) of Thailand for HRMS measurements.

References and notes

1. Schwab, P. F. H.; Smith, J. R.; Michel, J. *Chem. Rev.* **2005**, *105*, 1197–1279.
2. Sonntag, M.; Strohriegl, P. *Chem. Mater.* **2004**, *16*, 4736–4742.
3. Geng, Y.; Chen, A. C. A.; Ou, J. J.; Chen, S. H. *Chem. Mater.* **2003**, *15*, 4352–4360.
4. Katz, H. E.; Bae, Z.; Gilat, S. L. *Acc. Chem. Res.* **2001**, *34*, 359–369.
5. Cravino, A.; Roquet, S.; Aleveque, O.; Leriche, P.; Frere, P.; Roncali, J. *Chem. Mater.* **2006**, *18*, 2584–2590.
6. Mazzeo, M.; Pisignano, D.; Favaretto, L.; Barbarella, G.; Cingolani, R.; Gigli, G. *Synth. Met.* **2003**, *139*, 671–673.

7. Li, Z. H.; Wong, M. S.; Fukutani, H.; Tao, Y. *Chem. Mater.* **2005**, *17*, 5032–5040.
8. Wei, Y.; Wang, B.; Wang, W.; Tain, J. *Tetrahedron Lett.* **1995**, *36*, 665–668.
9. Tabet, A.; Schröder, A.; Hartmann, H.; Rohde, D.; Dunsch, L. *Org. Lett.* **2003**, *5*, 1817–1820.
10. Guyard, L.; Dumas, C.; Miomandre, F.; Pansu, R.; Renault-Méallet, R.; Audebert, P. *New J. Chem.* **2003**, *27*, 1000–1006.
11. Aso, Y.; Okai, T.; Kawaguchi, Y.; Otsubo, T. *Chem. Lett.* **2001**, 420–421.
12. Noda, T.; Imae, I.; Noma, N.; Shirota, Y. *Adv. Mater.* **1997**, *9*, 239–241.
13. Bäuerle, P.; Segelbacher, U.; Maier, A.; Mehring, M. *J. Am. Chem. Soc.* **1993**, *115*, 10217–10223.
14. Remonen, T.; Hellberg, J.; Slätt, J. *Synth. Met.* **1999**, *101*, 107–108.
15. Hotta, S.; Lee, S. A.; Tamaki, T. *J. Heterocycl. Chem.* **2000**, *37*, 281–290.
16. Meng, H.; Zheng, J.; Lovinger, A. J.; Wang, B.-C.; Van Patten, P. G.; Bao, Z. *Chem. Mater.* **2003**, *15*, 1778–1787.
17. Wong, K.-T.; Wang, C.-F.; Chou, C. H.; Su, Y. O.; Lee, G.-H.; Peng, S.-M. *Org. Lett.* **2002**, *4*, 4439–4442.
18. Yang, L.; Feng, J.-K.; Ren, A.-M. *J. Mol. Struc.: THEOCHEM* **2006**, *758*, 29–39.
19. Promarak, V.; Pankvuang, A.; Meunmat, D.; Sudyoadsuk, T.; Saengsuwan, S.; Keawin, T. *Tetrahedron Lett.* **2007**, *48*, 919–923.
20. *General procedure for coupling*: A mixture of bromo compound (0.536 mmol), $NiCl_2$ (0.95 g, 7.40 mmol), Zn (26 mg, 0.46 mmol), PPh_3 (39 mg, 0.15 mmol), and bipyridine (bpy) (12 mg, 0.08 mmol) in anhydrous DMAc (8 ml) was degassed with N_2 for 10 min. The reaction mixture was stirred at 90 °C under an N_2 atmosphere for 20 h. Purification was achieved by column chromatography over silica gel eluting with a mixture of CH_2Cl_2 and hexane followed by recrystallization with a mixture of CH_2Cl_2 and methanol.
Characterization data: **BFT2**: mp 126 °C; IR (KBr) 2927, 1599, 1493, 1467, 1212, 1054, 809, and 691 cm^{-1}; ^1H NMR (300 MHz, $CDCl_3$) δ 0.67–0.70 (8H, m), 0.79 (12H, t, $J = 6.4$ Hz), 1.09–1.17 (24H, m), 2.02 (8H, t, $J = 8.1$ Hz), 7.24 (2H, d, $J = 3.0$ Hz), 7.34–7.38 (8H, m), 7.58 (2H, s), 7.61 (2H, d, $J = 7.8$ Hz), and 7.71 (4H, d, $J = 7.8$ Hz); ^{13}C NMR (75 MHz, $CDCl_3$) δ 13.97, 22.56, 23.74, 29.69, 31.42, 40.42, 55.18, 119.71, 119.83, 120.09, 122.88, 123.58, 124.40, 124.51, 126.84, 127.16, 132.80, 136.47, 140.58, 140.90, 143.93, 150.91, and 151.60; HRMS-ESI m/z: [MH^+] calcd for $C_{58}H_{71}S_2$, 831.4992; found, 831.4976.
BFT4: mp 155 °C; IR (KBr) 2927, 1593, 1493, 1457, 1212, 1064, 879, and 691 cm^{-1}; ^1H NMR (300 MHz, $CDCl_3$) δ 0.67–0.73 (8H, m), 0.79 (12H, t, $J = 6.8$ Hz), 1.09–1.17 (24H, m), 2.02 (8H, t, $J = 8.0$ Hz), 7.14 and 7.16 (4H, AA′BB′, $J = 3.6$ Hz), 7.20 (2H, d, $J = 3.6$ Hz), 7.32–7.38 (8H, m), 7.57 (2H, s), 7.60 (2H, d, $J = 8.0$ Hz) and 7.70 (4H, d, $J = 7.9$ Hz); ^{13}C NMR (75 MHz, $CDCl_3$) δ 13.98, 22.56, 23.73, 29.69, 31.47, 40.40, 55.18, 119.74, 119.83, 120.08, 122.71, 122.88, 124.57, 124.89, 125.06, 126.82, 127.22, 132.90, 135.82, 136.57, 139.18, 149.52, 141.25, 144.68, 150.94, and 151.65; HRMS-ESI m/z: [MH^+] calcd for $C_{66}H_{75}S_4$, 995.4746; found, 995.4752.
BFT6: mp 231 °C; IR (KBr) 2927, 1599, 1493, 1470, 1213, 1152, 1056, 859, and 693 cm^{-1}; ^1H NMR (300 MHz, $CDCl_3$) δ 0.66–0.69 (8H, m), 0.78 (12H, t, $J = 7.0$ Hz), 1.08–1.17 (24H, m), 2.02 (8H, t, $J = 8.2$ Hz), 7.12 (8H, d, $J = 8.1$ Hz), 7.21 (2H, s), 7.32–7.39 (8H, m), 7.57 (2H, s), 7.59 (2H, d,$J = 8.2$ Hz), and 7.70 (4H, d, $J = 8.0$ Hz); ^{13}C NMR (75 MHz, $CDCl_3$) δ 13.96, 22.54, 23.73, 29.67, 31.46, 40.40, 55.18, 110.87, 119.73, 119.85, 120.10, 122.88, 123.57, 123.71, 124.06, 124.53, 124.70, 124.80, 125.15 126.84, 127.20, 132.59, 134.90, 135.68, 136.87, 138.67, 140.43, 141.03, 144.51, 150.90, and 151.61; HRMS-ESI m/z: [MH^+] calcd for $C_{74}H_{79}S_6$, 1159.4501; found, 1159.4491.
Oligothiophene **4**: ^1H NMR (300 MHz, $CDCl_3$) δ 0.66–0.69 (4H, m), 0.78 (6H, t, $J = 6.8$ Hz), 1.08–1.16 (12H, m), 2.01 (4H, t, $J = 8.1$ Hz), 6.94 (1H, d, $J = 3.6$ Hz), 7.00 (1H, d, $J = 3.9$ Hz), 7.04 (1H, d, $J = 3.6$ Hz), 7.09 (1H, d, $J = 3.6$ Hz), 7.13 and 7.14 (2H, AA′BB′, $J = 3.6$ Hz), 7.19 (1H, d, $J = 3.6$ Hz), 7.31–7.37 (4H, m), 7.56 (1H, s), 7.59 (1H, d, $J = 8.0$ Hz), and 7.70 (2H, d, $J = 7.8$ Hz); ^{13}C NMR (75 MHz, $CDCl_3$) δ 13.96, 22.55, 23.73, 29.67, 31.46, 40.39, 55.18, 110.80, 119.73, 119.84, 120.10, 122.88, 123.59, 123.62, 123.59, 123.79, 124.16, 124.30, 124.59, 124.73, 126.84, 127.20, 130.73, 132.60, 133.72, 135.88, 136.45, 136.89, 138.41, 140.71, 141.22, 145.90, 150.92, and 151.62; HRMS-ESI m/z: [MH^+] calcd for $C_{41}H_{42}BrS_4$, 741.1347; found, 741.1323.
21. Frisch, M. J.; Trucks, G. W.; Schlegel, H. B.; Scuseria, G. E.; Robb, M. A.; Cheeseman, J. R.; Zakrzewski, V. G.; Montgomery, J. A., Jr.; Stratmann, R. E.; Burant, J. C.; Dapprich, S.; Millam, J. M.; Daniels, A. D.; Kudin, K. N.; Strain, M. C.; Farkas, O.; Tomasi, J.; Barone, V.; Cossi, M.; Cammi, R.; Mennucci, B.; Pomelli, C.; Adamo, C.; Clifford, S.; Ochterski, J.; Petersson, G. A.; Ayala, P. Y.; Cui, Q.; Morokuma, K.; Malick, D. K.; Rabuck, A. D.; Raghavachari, K.; Foresman, J. B.; Cioslowski, J.; Ortiz, J. V.; Stefanov, B. B.; Liu, G.; Liashenko, A.; Piskorz, P.; Komaromi, I.; Gomperts, R.; Martin, R. L.; Fox, D. J.; Keith, T.; Al-Laham, M. A.; Peng, C. Y.; Nanayakkara, A.; Gonzalez, C.; Challacombe, M.; Gill, P. M. W.; Johnson, B. G.; Chen, W.; Wong, M. W.; Andres, J. L.; Head-Gordon, M.; Replogle, E. S.; Pople, J. A. GAUSSIAN *98, Revision A.7*; Gaussian: Pittsburgh, PA, 1998.
22. Thiem, H.; Strohriegl, P.; Setayesh, S.; de Leeuw, D. *Synth. Met.* **2006**, *156*, 562–589.
23. Jaramillo-Isaza, F.; Turner, M. L. *J. Mater. Chem.* **2006**, *16*, 83–89.
24. Bäuerle, P.; Würthner, F.; Götz, G.; Effenberger, F. *Synthesis* **1993**, 1099–1103.
25. Nakayama, J.; Konishi, T.; Marubayashi, S.; Hoshino, M. *Heterocycles* **1987**, *26*, 1793–1796.
26. Martinez, F.; Voelkel, R.; Naegele, D.; Naarmann, H. *Mol. Cryst. Liq. Cryst.* **1989**, *167*, 227–235.
27. Kartens, T.; Kobs, K. *J. Phys. Chem.* **1980**, *84*, 1871–1872.